Journal of Aerospace Technology and Management
ISSN: 2175-9146
Departamento de Ciência e Tecnologia Aeroespacial

Thannickal, Varghese M; Tharakan, T John; Chakravarthy, Satyanarayanan R

Stability Characteristics of a Model Trim Adjustment System
for Open Loop Active Control of Thermoacoustic Instability

Journal of Aerospace Technology and Management, vol. 11, e1019, 2019
Departamento de Ciência e Tecnologia Aeroespacial

DOI: https://doi.org/10.5028/jatm.v11.979

Available in: https://www.redalyc.org/articulo.oa?id=309457690004

https://doi.org/10.5028/jatm.v11.979 ORIGINAL PAPER

Stability Characteristics of a Model Trim Adjustment System for Open Loop Active Control of Thermoacoustic Instability

Varghese M Thannickal*[1], T John Tharakan[2], Satyanarayanan R Chakravarthy[3]

Thannickal VM http://orcid.org/0000-0003-2335-8905
Tharakan TJ http://orcid.org/0000-0001-6852-7528
Chakravarthy SR http://orcid.org/0000-0003-1178-6945

How to cite

Thannickal VM; Tharakan TJ; Chakravarthy SR (2019) Stability Characteristics of a Model Trim Adjustment System for Open Loop Active Control of Thermoacoustic Instability. J Aerosp Technol Manag, 11: e1019. https://doi.org/10.5028/jatm.v11.979

ABSTRACT: Thermoacoustic instability in liquid rocket engines can have potentially catastrophic consequences. Active control based on feedback promises improved stability margin over a wider range of operating conditions than passive control. In the present work, the thermoacoustic characteristics of a trim adjustment active control system based on variable volume tunable Helmholtz resonator are investigated in open loop. The effect of variation of parameters for a ducted resonator in relation to a duct alone is brought out for the fundamental and first harmonic mode in a closed-open duct using a mode tracking technique. Thermoacoustic instability of the first harmonic is predicted for lean mixtures. Combustion delay has an optimum with regard to the combustion stability of the flame in a duct. Introduction of the resonator stabilizes the fundamental mode completely with respect to flame position. Increasing the volume of the resonator is destabilizing for both fundamental and harmonic modes in fuel rich mixtures. The resonator has maximum effect in controlling instability when placed near the antinode of the standing wave pattern and when its characteristic frequency matches the modal frequency. Volume variable resonators are seen to be effective for control of thermoacoustic instability in open loop.

KEYWORDS: Trim adjustment, Open loop active control, Thermoacoustic characteristics, Combustion modes, Growth rate, Frequency.

INTRODUCTION

Thermoacoustic instability is a phenomenon observed sometimes in combustion systems such as rocket engines and gas turbines (Harrje and Reardon 1972; Yang and Andersen 2000; Lieuwen and Yang 2005), wherein the acoustic disturbances in the chamber couple with the heat release perturbations. This leads to pressure oscillations that can grow with time. The consequences of these oscillations are sometimes beneficial in terms of increased rates of chemical reaction and reduced pollutant emission (McManus *et al.* 1990; Yu *et al.* 1991). However, in gas turbines and rocket engines, they are likely to be highly destructive (Sewell and Sobieski 2005; Oefelein and Yang 1993).

Thermoacoustic instability can be controlled by decoupling the processes of heat release and acoustic wave propagation. The method used widely for this is by means of passive control (Richards *et al.* 2003). This is achieved by the introduction of static

1.Liquid Propulsion Systems Centre – Combustion Analysis and Research Facility – Propulsion Research and Studies – Thiruvananthapuram – India.
2.Liquid Propulsion Systems Centre – Propulsion Research Group – Propulsion Research and Studies – Thiruvananthapuram – India.
3.Indian Institute of Technology Madras – National Centre for Combustion Research and Development – Department of Aerospace Engineering – Chennai – India.
*Correspondence author: vargg100@gmail.com
Received: Nov. 22, 2017 | Accepted: Feb. 27, 2018
Section Editor: Dimitrius Pavlou

elements such as baffles, slots, liners, and resonators in the combustion chamber. These elements alter the acoustic boundary conditions in the chamber to achieve the required decoupling. However, experiments have been conducted in non-reactive systems that indicate that the stability of passive control systems degrade significantly under off-design conditions (Corá *et al.* 2014).

In order to counteract the disadvantages of passive control, active control is being extensively investigated (Annaswamy and Ghoniem 2002; Dowling and Morgans 2005; McManus *et al.* 1993. Active control makes use of a feedback loop to neutralize unstable disturbances. An active control system is said to be in closed loop or open loop depending on whether the feedback loop is activated or not. In this technique, the control elements, or actuators, are dynamic in nature. Conventionally, the control is effected by secondary fuel injection (Sattinger *et al.* 2000) or anti-sound (Williams 1984) that introduces heat or pressure perturbations respectively, out of phase with the instability. Such a control is classified as fast-response active control, since the actuation of the fuel injection or anti-sound is at the same time scale as that of the instability.

In liquid rockets, fuel injection valves cannot respond at the typically kilohertz range of frequencies of the instability, while anti-sound is impracticable in the high temperature and pressure conditions of the combustor. To overcome these difficulties, active control using tunable Helmholtz resonators has been proposed (Zhang *et al.* 2015; Zhao and Morgans 2009). This is referred to as trim adjustment control as opposed to the fast-response active control, in that the control element (resonator) needs to respond only at a time scale that is much slower than that of the instability. Here, the resonator responds only at the relatively slow rate of variation in the operating conditions. In practice, a variable cavity volume resonator would be easier to realize, as the actuator mechanism is simpler; therefore, it is considered here. Such variable volume resonators have been widely used in noise control applications (Estève and Johnson 2005; Bedout *et al.* 1997).

The design of a practical active controller can be achieved based on the knowledge of the thermoacoustic characteristics of the combustor, by treating the thermoacoustic system together with the controller as an eigenvalue problem and deriving the frequency and growth rate of the pressure perturbations. The thermoacoustic characteristics can be used to obtain the stability boundaries of the system. A control algorithm can then be configured to determine how far away the operating point is from the stability boundary and take appropriate corrective action.

As a prelude to identifying a control algorithm, the present work aims to characterize the open loop thermoacoustic characteristics of a trim adjustment active control system based on a variable volume tunable Helmholtz resonator. The corresponding characteristics of the ducted resonator, i.e., the combustor duct with the Helmholtz resonator, are compared with those of the combustor duct without the resonator, as the system parameters are varied. The frequency and growth rate are presented as a function of the combustion gain as the time delay and other system parameters are varied.

The eigenvalue technique of determining the characteristics of thermoacoustic systems has been commonly adopted by many investigators, either in the classical formulation (McManus *et al.* 1993) or the more recent cluster treatment of characteristic roots (CTCR) paradigm (Olgac *et al.* 2014; Zalluhoglu and Olgac 2016). However, the classical technique has not been applied to determine the thermoacoustic characteristics of tunable Helmholtz resonator systems, while the CTCR paradigm has been applied for only fixed geometry resonators so far. Also, in the earlier work on active control by tunable Helmholtz resonators too (Zhang *et al.* 2015; Zhao and Morgans 2009), the focus was on numerical computations in the time domain using different flame models, but the characteristics in the frequency domain are not explored. The present approach of mode tracking is a novel method of determining the thermoacoustic characteristics in the frequency domain in a rigorous manner.

Applying the eigenvalue technique to determine the open loop thermoacoustics is a simple yet elegant approach for trim adjustment active control based on a tunable Helmholtz resonator. The present work develops the general framework for such an analysis and explicitly explores the dependencies of all the governing parameters so as to form the basis for devising an algorithm to eventually implement the control on practical combustor hardware.

MATHEMATICAL FORMULATION

A liquid rocket engine thruster comprises injectors to deliver the fuel and oxidizer, the combustion chamber where mixing and chemical reaction takes place, followed by the nozzle. Despite the complex geometry of such a combustor and the associated

processes, it is not uncommon to adopt a simplified geometry and a set of assumptions for the present purpose (Chen *et al.* 2016; Li and Morgans 2015; Surendran *et al.* 2016). Adopting such a framework would enable faster, real time implementation of a control algorithm that can be developed from the model such as the present one.

Accordingly, the simplified configuration adopted in the present work representing a liquid rocket engine combustor subjected to a trim adjustment active control system in open loop is shown in Fig. 1. The combustor is taken as a duct with one end closed and the other end open. A mixture of fuel and oxidizer is admitted at the closed end of the duct and burns at a thin flame located axially downstream at a distance x_f from the closed end, and its combustion products exit through the open end of the duct. Longitudinal mode acoustic oscillations are considered for control in the present work. Although liquid rocket motors are prone to high frequency tangential/radial modes as well, this is a representative consideration to theoretically demonstrate the open loop controllability of acoustic oscillations in a given longitudinal mode and could be extended to other modes later. A tunable Helmholtz resonator with variable geometry is the control element located on the wall at a distance x_h from the flame in the axial direction.

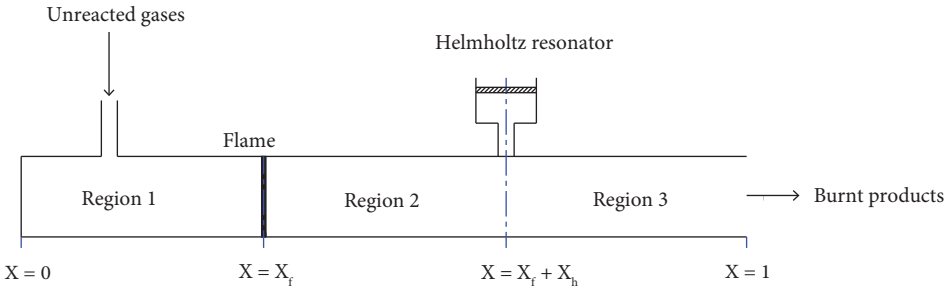

Figure 1. Schematic of open loop trim adjustment active control using tunable Helmholtz resonator.

The mean flow is neglected in comparison to the speed of sound, and the effect of grazing flow on the resonator damping is also neglected in the first approximation. In a rocket motor the first assumption is well justified while grazing flow effects can be accommodated by suitable correlations. The combustor is divided into three regions numbered as 1, 2, and 3, separated by the thin flame and the location of the resonator, as indicated in Fig. 1. The temperature, density, speed of sound, and acoustic impedance are denoted by T, ρ, c, and Z respectively.

A linear analysis is performed to characterize the trim adjustment control system. The variables are non-dimensionalized at the start of the analysis as follows: the spatial coordinate, velocity, and pressure are non-dimensionalized with respect to the duct length L, thermodynamic speed of sound c at the mean temperature of the unburnt medium, and $\gamma\overline{P}$ respectively, where γ is the ratio of specific heats and $\overline{P}$ is the mean chamber pressure. Accordingly, time is non-dimensionalised by the characteristic acoustic time, L/c. The volumetric heat release rate is non-dimensionalized by $\gamma\overline{P}/(\gamma - 1)$. The properties of the burnt medium are normalized with respect to the same quantities as in the unburnt medium, but taking the values corresponding to the burnt mixture.

The governing equations are written down separately for each region of the duct and transformed into the frequency domain. The transformation is achieved by assuming, without loss of generality, that all the fluctuating variables are temporally of sinusoidal form, i.e.,

$$v(x,t) = V(x)\exp(-i\omega t) \tag{1}$$

where: t is time, x is the spatial coordinate, and $v(x,t)$ is any fluctuating variable. $V(x)$ is the spatial component of $v(x,t)$, and ω is the frequency of variation of $v(x,t)$, which are, in general, complex. Since $\omega = \omega_r + i\omega_i$, where ω_r is the real part of the complex frequency and ω_i is the imaginary part, it follows that the observed frequency of the thermoacoustic oscillations is ω_r and their growth rate is ω_i by substitution in Eq. 1.

The system matrix is successively constructed from the thermoacoustics of the duct and the resonator dynamics. The system thermoacoustic characteristics are then derived from the system matrix as an eigenvalue problem. As we are considering open loop behavior in the present case, the controller characteristics will not be included in the analysis.

FORMULATION OF THE SYSTEM MATRIX

The system matrix is formed by considering the acoustics of the duct, combustion across a thin flame, and the resonator dynamics, all in the frequency domain. The frequency domain solution of the wave equation with negligible mean flow is given by (Eqs. 2 and 3) (Jacobsen 2000)

$$P(x) = P_R \exp\{ik(x - x_f)\} + P_L \exp\{-ik(x - x_f)\} \tag{2}$$

$$U(x) = \frac{P_R}{\rho c} \exp\{ik(x - x_f)\} - \frac{P_L}{\rho c} \exp\{-ik(x - x_f)\} \tag{3}$$

where P and U are the amplitudes of pressure and velocity in the frequency domain respectively, and ρ is the mean density of the medium. Subscripts R and L denote the right and left running waves in the duct, and $k = \omega/c$ is the wave number.

Realistic modeling of the flame involves correlating the burning area to the flow parameters. However, the heat release by the flame can be represented by the two parameter model (Crocco 1965), which in the frequency domain is (Eq. 4)

$$Q = n\,U(x_f)\exp(i\omega\tau) \tag{4}$$

where n is the combustion gain and τ is the combustion delay.

The resonator is considered to have a variable volume from practical considerations with, to a good approximation, incompressible flow through it. The flow in the neck of the resonator is considered to be frictionless but having inertia. Assuming that the mean flow and body forces are negligible, the linearized continuity and momentum equations in the frequency domain for the resonator in open loop respectively become (Eqs. 5 and 6)

$$\frac{-i\omega \bar{V}_h}{\rho_j c_j^2} P_h = \bar{A}_h U_h \tag{5}$$

$$P_j - P_h = -i\omega \rho_j l_h U_h \tag{6}$$

The system matrix is formulated by imposing boundary and interface conditions on the governing equations as follows:

- Zero velocity perturbation at the closed inlet (Eq. 7),

$$U(0) = 0 \tag{7}$$

- Zero pressure perturbation at the open outlet (Eq. 8),

$$P(1) = 0 \tag{8}$$

- Pressure continuity at a thin flame (Eq. 9),

$$P(x_f+) = P(x_f-) \tag{9}$$

- Heat release across a thin flame (Eq. 10) (McManus *et al.* 1993):

$$Q = U(x_f+) - U(x_f-) \tag{10}$$

- Pressure continuity at the resonator (Eq. 11):

$$P(x_h+) = P(x_h-) \tag{11}$$

- Flow continuity at the resonator (Eq. 12):

$$U(x_h-) = \varepsilon_A U_h + U(x_h+) \tag{12}$$

In Eqs. 9 to 12, + represents the region just after the flame and – the region just before it. ε_A is the ratio of the resonator neck area to the duct cross-sectional area. The governing equations of the resonator, Eqs. 5 and 6, and the boundary and interface conditions of the duct, Eqs. 7 to 12, can be combined to form the matrix that governs the system behavior.

The system matrix is explicitly written out for two cases that are distinctly considered in the next section, one being the combustor duct without the resonator and the other the ducted resonator. The thermoacoustic characteristics viz. frequency and growth rate are determined by equating the determinant of the system matrix to zero and solving for the real and imaginary parts of the complex frequency respectively assuming purely sinusoidal disturbances.

If the operating point lies outside the regions in parameter space where the growth rate is zero, some form of control is necessary. In the present analysis, the thermoacoustic characteristics are expressed as a function of combustion gain as time delay and other governing parameters are varied.

THERMOACOUSTIC CHARACTERISTICS

As mentioned above, two cases are considered: first, the case of the combustor duct alone, i.e., the duct with the flame but without the resonator; and the next is that of the ducted resonator. Considering the two cases distinctly allows for comparison on the effect of the open loop control by the resonator.

DUCT ALONE

Imposing the conditions pertaining to the combustor duct alone, Eqs. 7 to 10, the system matrix can be derived and the governing equation for the stability boundary determined as (Eq. 13) (McManus *et al.* 1993)

$$-N\sin(\theta_1)\sin(\theta_2) + \frac{1}{Z_2}\cos(\theta_1)\cos(\theta_2) \quad = 0 \tag{13}$$

where $N = 1 + n\exp(i\omega\tau)$, $\theta_1 = \omega xf$, and $\theta_2 = \omega\,(1 - x_f)/c_2$.
Here $c_2 = \sqrt{T_2}$ and $Z_2 = 1/\sqrt{T_2}$, which is valid for low Mach number flows, assuming that the mixture molecular weight and γ do not change significantly across the flame.

The value of T_2 can be related to the combustion gain, n, by taking the energy balance across the flame (Eq. 14):

$$q = \rho V u c_p T\,(T_2 - 1) \tag{14}$$

where q is the heat released in a small volume V enclosing the flame, u is the dimensional velocity of reactants entering the flame, ρ is their density, T is their temperature, while c_p is the specific heat at constant pressure. Substituting the equation of state, $\rho = (P/RT)$ in Eq. 14 and nondimensionalising the volumetric heat release, q/V, as per wthe earlier convention we obtain (Eq. 15)

$$Q = u'(T_2 - 1) \tag{15}$$

where we have assumed variables q, u and P to consist of small perturbations about a mean and linearized Eq. 14 taking mean velocity to be negligible as would be the case in rocket motors. Comparing the complex amplitudes of Eqs. 4 and 15, we readily obtain that $n = T_2 - 1$, a result that is consistently used to express T_2 in terms of n in the system matrix throughout the analysis. Equation 14 is a complex equation in ω, from which the thermoacoustic characteristics can be obtained by solving for ω and determining its real and imaginary parts.

OPEN LOOP STABILITY OF A TRIM ADJUSTMENT ACTIVE CONTROL SYSTEM

Now, consider the case where a variable geometry Helmholtz resonator is introduced into the duct, keeping the feedback loop open. Four additional equations pertaining to the resonator, Eqs. 5, 6, 11, 12, are introduced into the combustor duct matrix to form an 8 × 8 thermoacoustic system matrix (Eq. 16) corresponding to a 8 × 1 column vector of system variables $[P_{1R}\ P_{1L}\ P_{2R}\ P_{2L}\ P_{3R}\ P_{3L}\ P_h\ U_h]^{\mathrm{T}}$. Here, V is the ratio of volume of resonator to volume of chamber, and $\Omega = \sqrt{A_h/(V_h l_h)}$ is a characteristic frequency of the resonator divided by the local non-dimensional speed of sound, referred to simply as the resonator frequency.

$$\mathbf{M_T} = \begin{pmatrix} e^{-i\omega x_f} & -e^{i\omega x_f} & 0 & 0 & 0 & 0 & 0 & 0 \\ 0 & 0 & 0 & 0 & e^{\frac{i\omega(1-x_f)}{c_2}} & e^{\frac{-i\omega(1-x_f)}{c_2}} & 0 & 0 \\ 1 & 1 & -1 & -1 & 0 & 0 & 0 & 0 \\ -1-n\,e^{i\omega\tau} & 1+n\,e^{i\omega\tau} & \frac{1}{\rho_2 c_2} & -\frac{1}{\rho_2 c_2} & 0 & 0 & 0 & 0 \\ 0 & 0 & e^{\frac{i\omega x_h}{c_2}} & e^{-\frac{i\omega x_h}{c_2}} & -e^{\frac{i\omega x_h}{c_2}} & -e^{-\frac{i\omega x_h}{c_2}} & 0 & 0 \\ 0 & 0 & e^{\frac{i\omega x_h}{c_2}} & e^{-\frac{i\omega x_h}{c_2}} & 0 & 0 & -1 & \frac{i\omega\rho_2}{\Omega^2} \\ 0 & 0 & e^{\frac{i\omega x_h}{c_2}} & -e^{-\frac{i\omega x_h}{c_2}} & -e^{\frac{i\omega x_h}{c_2}} & e^{-\frac{i\omega x_h}{c_2}} & 0 & -V \\ 0 & 0 & 0 & 0 & 0 & 0 & \frac{\omega}{\rho_2 c_2^2} & -i \end{pmatrix} \quad (16)$$

The thermoacoustic characteristics are derived from the above 8 × 8 system matrix by taking the determinant as before and equating to zero, solving for complex frequency and thereby obtaining the growth rate and frequency.

RESULTS AND DISCUSSION

MODE DIAGRAM

It is seen from Eq. 14 that ω is a function of the combustion parameters n and τ as well as geometric parameters characterizing the system. A mode diagram is constructed by plotting the evolution of the imaginary part of ω (the growth rate) and its real part (the frequency) against the combustion gain, at different values of τ and geometric parameters, for a particular acoustic mode. This is done by starting an iteration with n = 0 and the desired mode acoustic frequency and calculating the mode growth rate and frequency as n is incremented in steps. The magnitude of the step is determined by grid independence considerations. A value of 0.01 was found to be adequate and used throughout this study. At each step the starting guess for the complex frequency is revised to the most recent complex frequency calculated. The additional geometric parameters present in Eq. 14 can also be varied to study their effect.

A typical mode diagram is given in Fig. 2 to explain the basic features qualitatively.

The mode is unstable when the growth rate is positive, i.e. along segment ABC in Fig. 2a. Conversely segment CDE in the same figure corresponds to stability of the mode. The margin of stability is given by the negative of the ordinate of the growth rate mode diagram and measures the degree of combustion stability of the system with respect to the selected mode. The ordinate at B and the abscissa at C also give an indication of the degree of instability of the mode in segment ABC. The greater these values the more unstable is the mode at the given τ and geometric parameters. Conversely the lesser the ordinate at D and the greater the width CE, the more stable is the mode in segment CDE. The frequency mode diagram, Fig. 2b, shows a typical behavior wherein, starting from the acoustic mode at n = 0, the system transitions to higher modes in a continuous fashion along ABC, reaching an asymptotic value at D corresponding to the acoustic frequency of a higher mode.

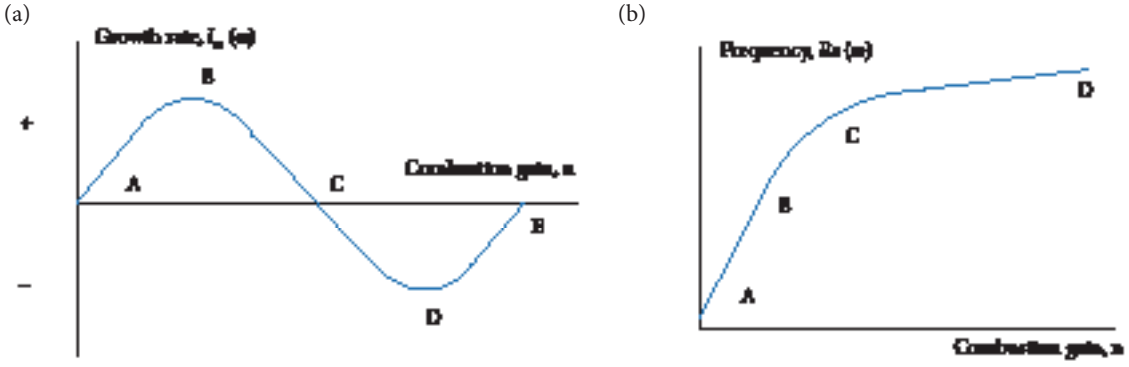

Figure 2. Schematic mode diagram showing (a) growth rate and (b) frequency (combustion delay and geometric parameters constant).

THERMOACOUSTIC CHARACTERISTICS FOR A DUCT

NOMINAL DUCT CHARACTERISTICS

Before investigating effect of resonator in open loop, it is necessary to study the characteristics of a duct for comparison. To quantify the effect of variation of τ and geometric parameters, the following nominal conditions are chosen and effect of varying one parameter at a time is analyzed: $\tau = 0.6$, $x_f = 0.1$. The nominal τ and x_f are typical of liquid rockets. The nominal thermoacoustic characteristics of a duct are given in Fig. 3 for the 1L mode and in Fig. 4 for the 3L mode.

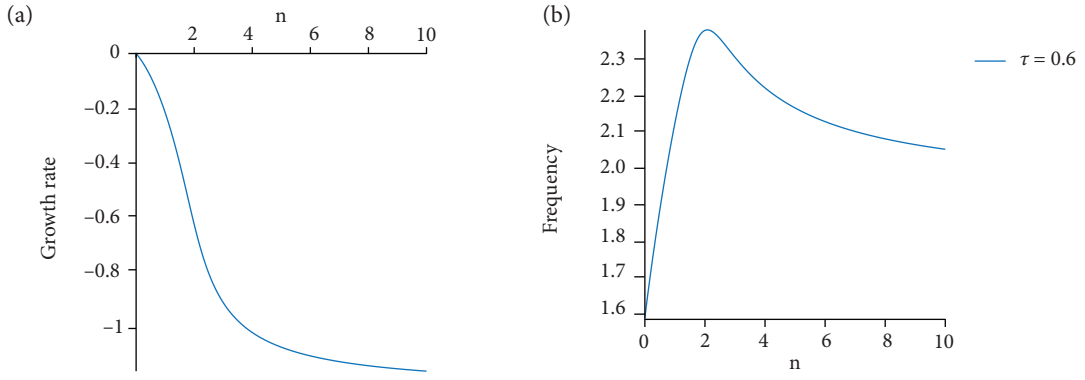

Figure 3. Nominal thermoacoustic characteristics for duct (1L mode) showing (a) growth rate and (b) frequency.

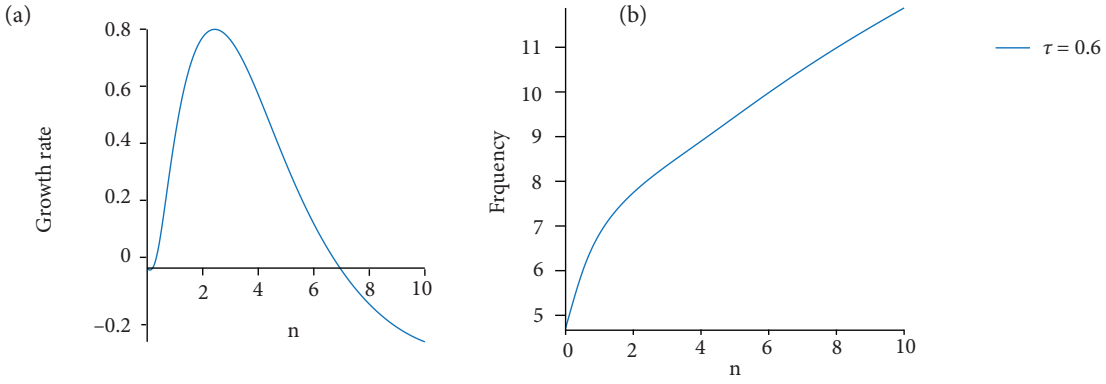

Figure 4. Nominal thermoacoustic characteristics for duct (3L mode) showing (a) growth rate and (b) frequency.

Both the growth rate and frequency characteristics are remarkably different for the two modes. 1L mode is always stable in the nominal condition whereas 3L mode is largely unstable. The frequency of the 1L mode remains near the fundamental non-dimensional acoustic frequency of $\pi/2$ whereas the frequency of the 3L mode ($3\pi/2$) transitions rapidly through non-dimensional acoustic frequencies of higher modes.

Effect of Variation of Combustion Time Delay

The thermoacoustic characteristics of a 1L mode in a duct combustor is shown in Fig. 5 as combustion gain and delay are varied. From Fig. 5a, the nominal condition is optimal from the point of view of stability. Off nominal conditions are more unstable and by $\tau = 1$, the system is largely unstable. This indicates that while moderately lean mixtures under rocket motor conditions are stable with respect to 1L mode, increasing the mixture ratio till the stoichiometric (n ~ 3-4) is detrimental to stability as τ increases. Thus there is an upper limit to the time delay for avoiding combustion instability as far as 1L mode is concerned. The reason for the destabilization is apparent in Fig. 5b where the mode transitions from 1L to 3L in a continuous manner and the 3L mode is shown below to be unstable under these conditions. A correlation is also observed between the slopes of the growth and frequency mode diagrams of Fig. 5 at different τ.

The corresponding mode diagrams for the 3L mode are given in Fig. 6. Increasing or decreasing the value of τ from the nominal, stabilizes the system. There is thus a range of v between 0.3 and 1.0 where the combustion in the duct is destabilized with respect to the 3L mode. For stability with respect to both the 1L and 3L modes in a duct combustor, it will be necessary to operate in approximately the range $0.3 < \tau < 0.45$ and any τ beyond 0.7 or less than 0.3 would lead to instability. This is to be expected from the Rayleigh criterion wherein combustion delay would have to lie in certain ranges relative to the acoustic time period for disturbances to be amplified or suppressed (McManus *et al.* 1990). In regard to frequency, the phenomenon of mode

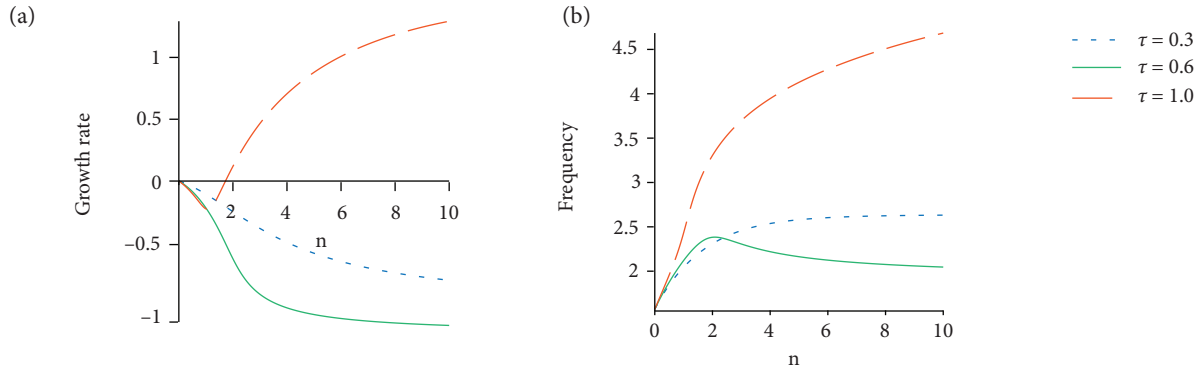

Figure 5. Thermoacoustic characteristics of a duct (1L mode, x_f = 0.10) showing (a) growth rate and (b) frequency.

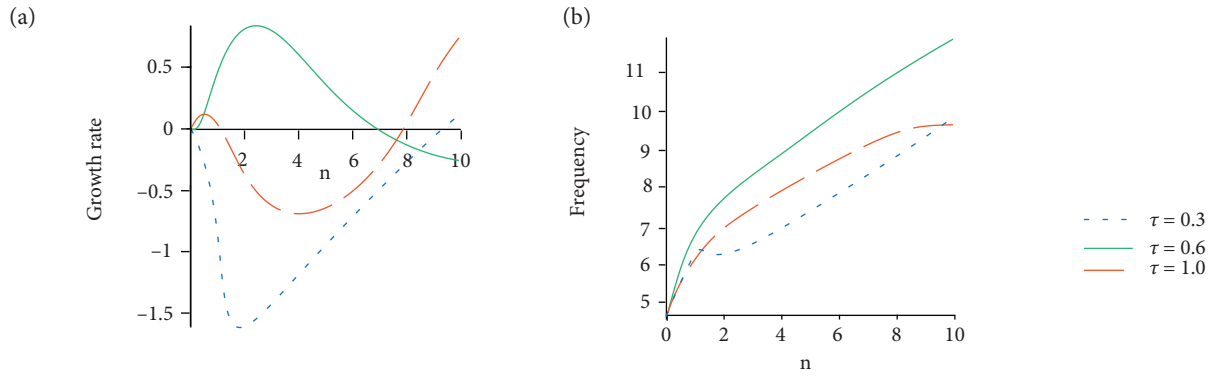

Figure 6. Thermoacoustic characteristics of a duct (3L mode, x_f = 0.10) showing (a) growth rate and (b) frequency.

transition is particularly marked for the 3L mode, the initially 3L mode transitioning beyond the next higher odd mode. Like 1L mode, correlations are seen between the trends in growth rate and frequency plots of the 3L mode.

EFFECT OF VARIATION OF FLAME POSITION

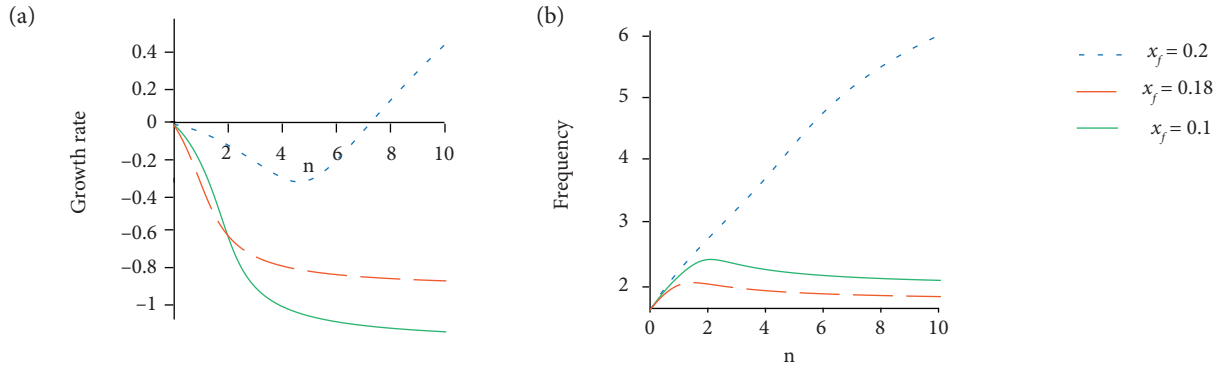

Figure 7. Thermoacoustic characteristics in a duct as flame position varies (1L mode, τ = 0.6) showing (a) growth rate and (b) frequency.

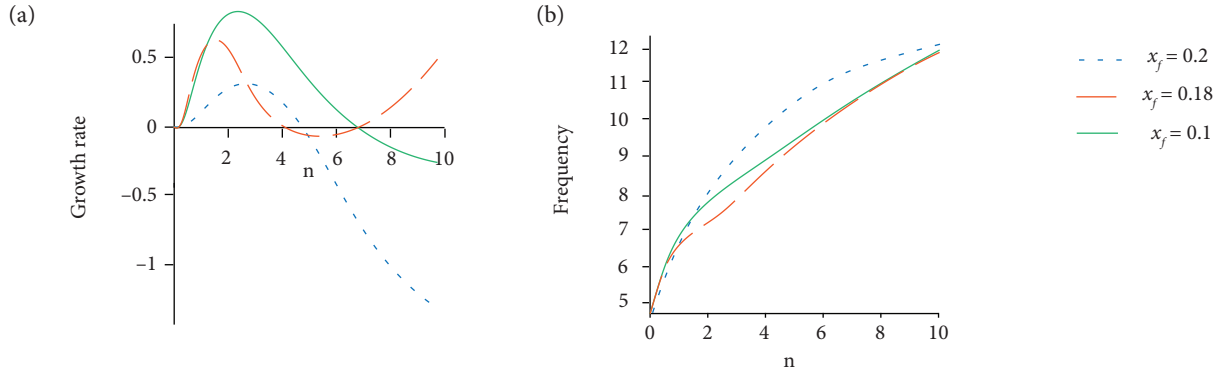

Figure 8. Thermoacoustic characteristics of a duct as flame position varies (3L mode, τ = 0.6) showing (a) growth rate and (b) frequency.

THERMOACOUSTIC CHARACTERISTICS OF DUCTED RESONATOR

NOMINAL THERMOACOUSTIC CHARACTERISTICS

The effect of introducing a resonator on nominal thermoacoustic characteristics is given in Fig. 9 for 1 L mode and Fig. 10 for 3L mode.

As in the case of the duct alone, the combustion delay and flame position are typical of liquid rocket motors. The nominal parameters of the resonator are chosen as $V = 0.2$, $\omega h = 2$ and $xh = 0.5$ so that the effect of the resonator is clearly brought out. From Fig. 9a, it is seen that addition of resonator shifts the inflection in the mode diagram to a higher value of n but the asymptotic value remains almost the same. Between $n = 2.5$ and 3.5 there is a rapid increase in stability of the ducted resonator with respect to 1L mode. The frequencies in the nominal condition for 1L mode (Fig. 9b) show similar behavior for both duct and ducted resonator. For the 3L mode (Fig. 10a), with the resonator there is a stabilization of the stable and unstable segments of the mode diagram. The 3L mode for the ducted resonator increases faster than the case with duct only (Fig. 10b).

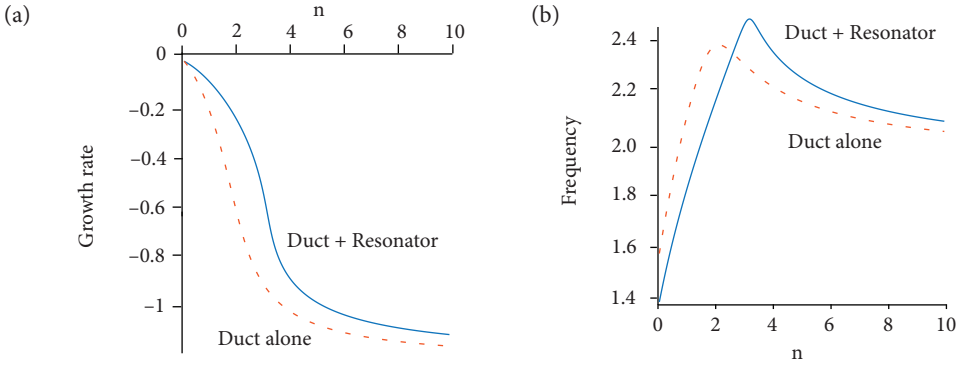

Figure 9. Nominal thermoacoustic characteristics of a ducted resonator (1L mode, $\tau = 0.6$, $x_f = 0.10$, $V = 0.2$, $\omega_h = 2$, $x_h = 0.5$) showing (a) growth rate and (b) frequency.

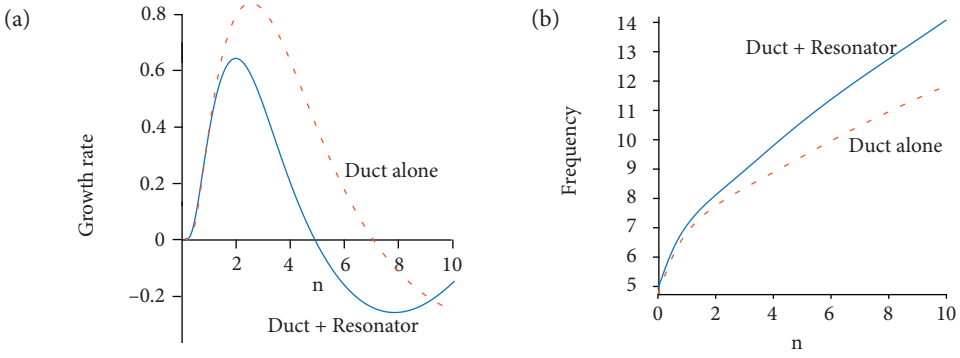

Figure 10. Nominal thermoacoustic characteristics of a ducted resonator (3L mode, $\tau = 0.6$, $x_f = 0.10$, $V = 0.2$, $\omega_h = 2$, $x_h = 0.5$) showing (a) growth rate and (b) frequency.

Effect of Variation of Combustion Time Delay

The effect of varying the combustion time delay on the thermoacoustic characteristics is given in Figs. 11 and 12 for the 1L and 3L modes, respectively. In Fig. 11 we see that the trends are similar to the case of duct alone when $x_f = 0.10$ and for $\tau \leq 0.6$. However, at the largest value of τ the width of the stable segment is increased by almost double, from n = 1.7 to n = 4, and the maximum stability margin decreases slightly at this value of time delay. Also a combustion process with a delay of $\tau = 1$ shows greater degree of stability in the unstable region when resonator is present, rather than duct alone. Figure 11 hence confirms that introduction of a resonator causes an improvement in overall stability with respect to the 1L mode, though the effect is more pronounced for $\tau > 0.6$. The frequency plots Fig. 7b and 11b are largely similar, with frequency transition from 1L to 3L seen in both at the highest τ.

Comparison of the 3L mode characteristics between duct alone (Fig. 6) and duct with resonator (Fig. 12) shows significant decrease in the width of the stable region for $\tau \leq 0.6$ and of the unstable region for $\tau = 1.0$. However the height of these regions remains the same. Hence for the 3L mode, introduction of the resonator decreases stability for $\tau \leq 0.6$ and increases stability for $\tau \cong 1.0$. This is to be contrasted with the behavior of 1L mode wherein the introduction of a resonator increases stability at all τ. The behavior of the frequency between duct alone and ducted resonator cases is essentially the same (Figs. 5b and 7b), though within the span of $0 < n < 10$ the frequencies for a ducted resonator transition faster with respect to n as compared to a duct alone.

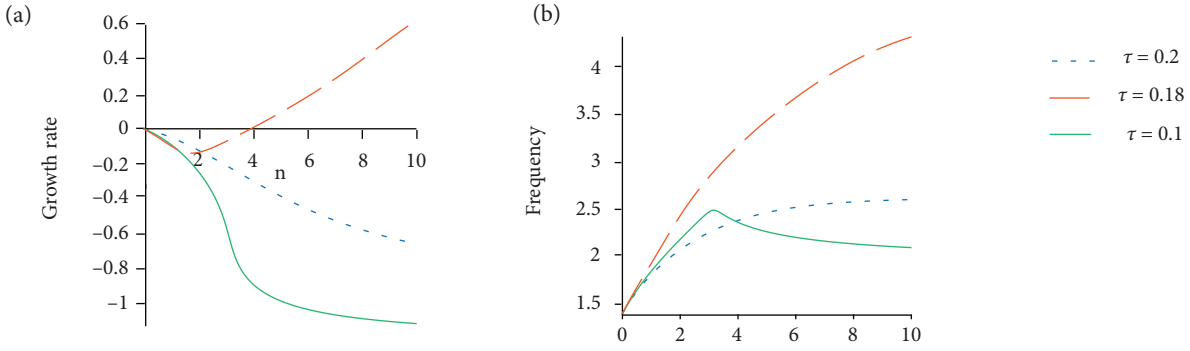

Figure 11. Thermoacoustic characteristics of a ducted resonator as combustion delay varies (1L mode, $x_f = 0.10$, $x_h = 0.5$, $V = 0.2$, $\omega_h = = 2$) showing (a) growth rate and (b) frequency.

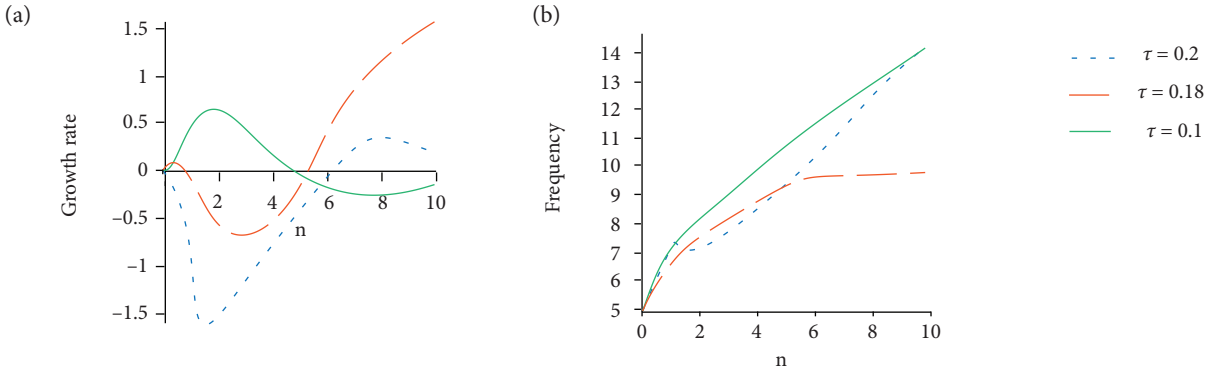

Figure 12. Thermoacoustic characteristics of a ducted resonator as combustion delay varies (3L mode, $x_f = 0.10$, $x_h = 0.5$, $V = 0.2$, $\omega_h = 2$) showing (a) growth rate and (b) frequency.

EFFECT OF VARIATION OF FLAME POSITION

The effect of variation of flame position is shown in Fig. 13 for the 1L mode and Fig. 14 for the 3L mode. These are to be compared to the corresponding plot for the duct alone given in Figs. 7 and 8. The combustion process is more fully stabilized by the introduction of a resonator for all the values of x_f considered. Similarly stability with respect to the 3L mode is also enhanced as x_f is varied from the nominal. The width of the region of stability when $x_f = 0.18$ is also increased. The comparison of the frequency mode diagrams for the 1L mode for both duct and ducted resonator (Figs. 7b and Fig. 13b) shows that for $x_f \leq 0.1$ the resonator has negligible impact whereas it slows down the rate of increase of frequency with n for $x_f = 0.18$. Thus the nominal resonator configuration chosen in this parametric survey is well tuned to the 1L mode at $x_f = 0.18$. The frequency diagrams for duct and ducted resonator (Figs. 8b and 14b) for 3L mode do not reveal significant effects due to variation in flame position.

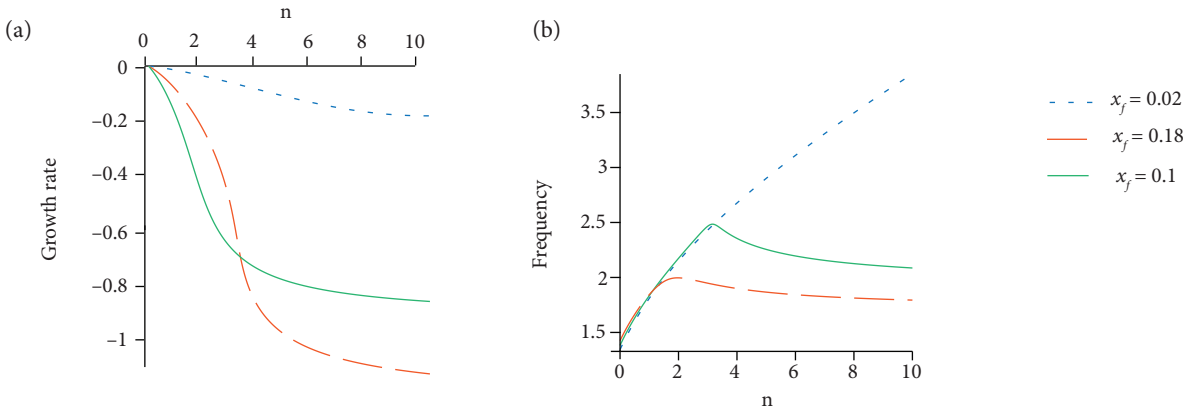

Figure 13. Thermoacoustic characteristics of a ducted resonator: as flame position varies (1L mode, $\tau = 0.6$, $x_h = 0.5$, $V = 0.2$, $\omega_h = 2$) showing (a) growth rate and (b) frequency.

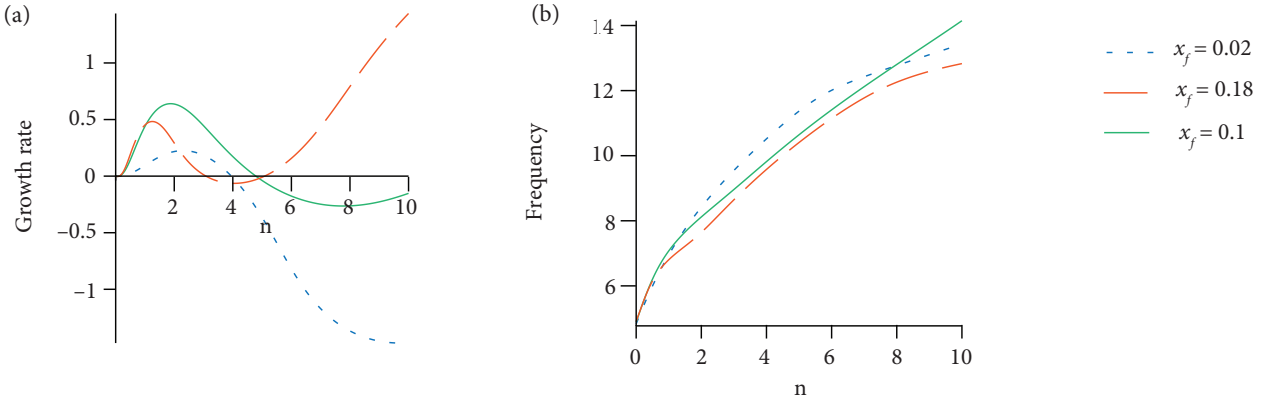

Figure 14. Thermoacoustic characteristics of a ducted resonator as flame position varies (3L mode. $\tau = 0.6$. $x_{i,} = 0.5$. $V = 0.2$. $\omega_{i,} = 2$) showing (a) growth rate and (b) frequency.

EFFECT OF VARIATION OF VOLUME RATIO

The effect of the volume ratio of the resonator is shown in Figs. 15 and Fig. 16 for 1L and 3L mode respectively. Numerical simulations show the effect of the resonator becomes apparent only after $V = 0.1$ and reaches a limiting value for large V as would be expected physically also. The effect of resonator is optimum when $0.1 < V < 0.3$, which may be achieved by a single resonator of larger size or by the use of multiple small resonators if space constraints exist.

Figure 15a shows that within the optimum range, a resonator of smaller volume has slightly greater stability margin. However as seen in Fig. 16a, the opposite is the case with the 3L mode for $n < 7$. By varying the flame position it may be possible to stabilize an initially unstable 3L mode over a narrow mixture ratio range, such that $4.2 < n < 5.5$. For $n < 4.2$ the combustion cannot the stabilized with respect to the 3L mode while for $n > 4.2$ the combustion can be made stable by suitably choosing the volume ratio. For $5.5 < n < 7$ there is a reversal in the stability characteristics of the 3L mode and it becomes more stable at a smaller volume ratio. The frequency plots for the 1L mode do not show any transitions while significant transitions are seen in the 3L mode, which are in line with what was observed in the nominal duct alone configuration.

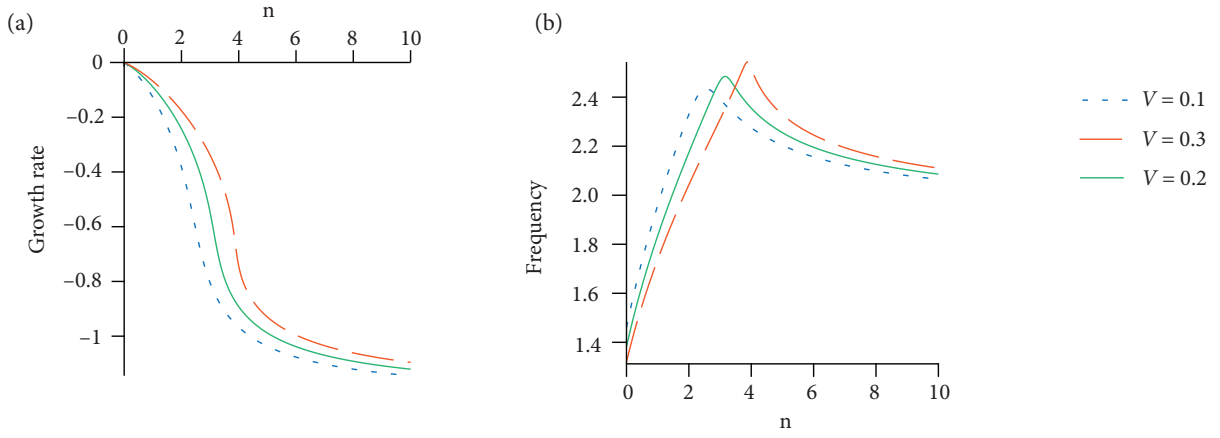

Figure 15. Thermoacoustic characteristics of a ducted resonator as volume ratio varies (1L mode, τ = 0.6, x_f =0.10, x_h = 0.5, ω_h = 2) showing (a) growth rate and (b) frequency.

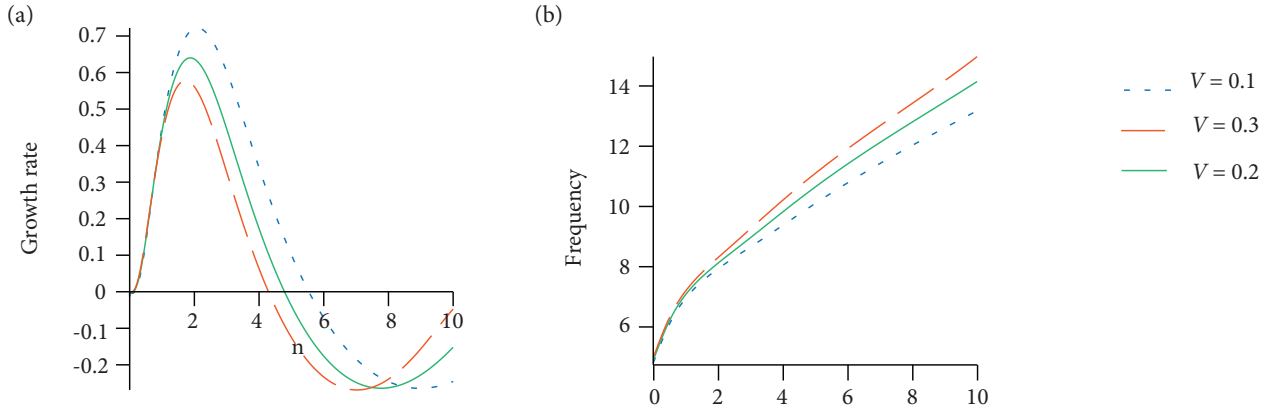

Figure 16. Thermoacoustic characteristics of a ducted resonator as volume ratio varies (3L mode, τ = 0.6, x_f = 0.10, x_h = 0.5, ω_h = 2) showing (a) growth rate and (b) frequency.

Effect of Variation of Resonator Position

The effect of varying resonator position is given in Fig. 17 for the 1L mode and Fig. 18 for the 3L mode. In Fig. 17, the effect of increasing xh on the 1L mode is to increase the margin of stability. For the 3L mode, there is seen to be an optimum resonator

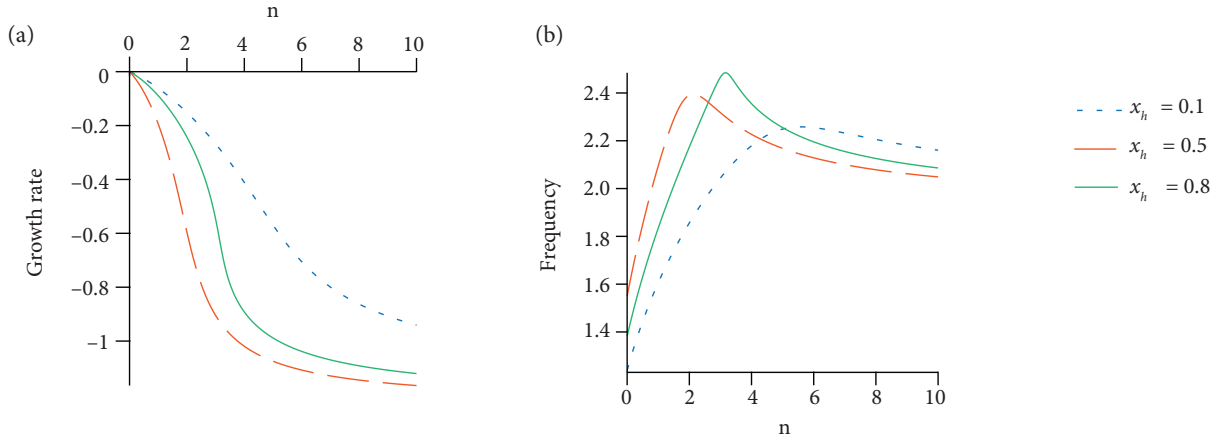

Figure 17. Thermoacoustic characteristics of a ducted resonator as resonator position varies (1L mode, τ = 0.6, x_f = 0.10, V = 0.2, ω_h = 2) showing (a) growth rate and (b) frequency.

position for maximum stability margin around half the length of the duct relative to the flame. This is close to an antinode of the standing wave pattern in the tube and is in line with the literature (Yang and Morgans 2016) on optimum location of the resonator.

No significant effects are observed due to the variation of xh on the frequency plot for 1L mode (Fig. 17b). The frequency diagrams for the 3L mode (Fig. 18b) shows that the trends are same as without a resonator but there exists an optimum position of resonator relative to the flame ($x_h = 0.5$) where the rate of growth of modal frequency with combustion gain is maximum and that this rate is greater than the nominal rate for a duct alone.

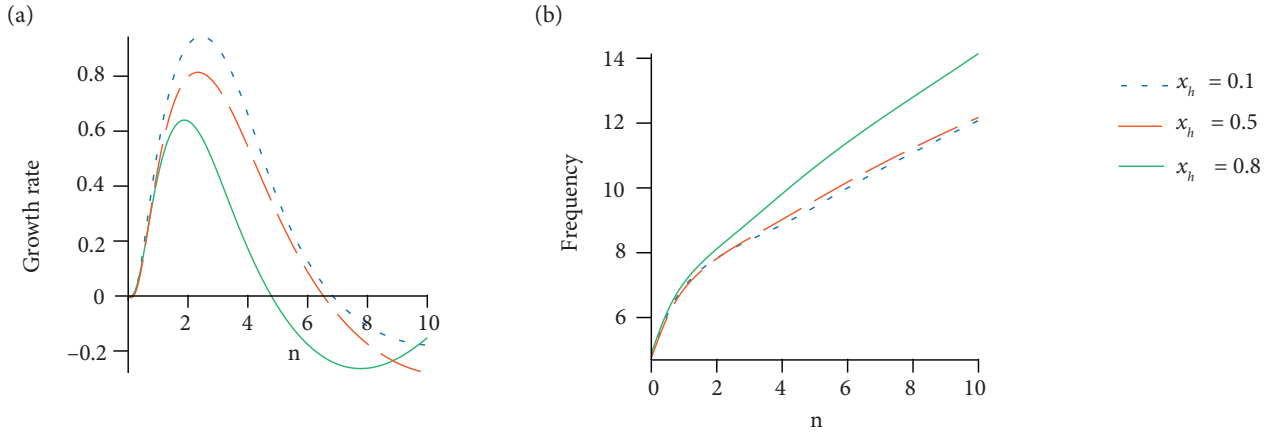

Figure 18. Thermoacoustic characteristics of a ducted resonator as resonator position varies (3L mode, $\tau = 0.6$, $x_f = 0.10$, $V = 0.2$, $\omega_h = 2$) showing (a) growth rate and (b) frequency.

EFFECT OF VARIATION OF RESONATOR FREQUENCY

The effect of resonator characteristic frequency is given in Figs. 19 for the 1L mode and Fig. 20 for the 3L mode. Varying the characteristic frequency shows that the lowest resonant frequency ($\omega_h = 1$) is most stable. Since the frequency of the 1L mode is around 2 (Fig. 19b) this is expected as $\omega_h c_2 = \omega_h \sqrt{(1 + n)} \approx 2$ and hence the resonator frequencies and the mode frequencies nearly match when $\omega_h = 1$. For the 3L mode, in the nominal condition, the extent of the unstable segment is decreased by the introduction of the resonator. A similar observation can be made for the stable region. The stabilizing effect is most pronounced for $\omega_h = 3$, which by a similar argument as for the 1L mode can be correlated to a coupling of resonator and duct at higher characteristic frequency for the higher frequency 3L mode. The frequency diagrams for the 1L mode (Fig. 19b) do not show any

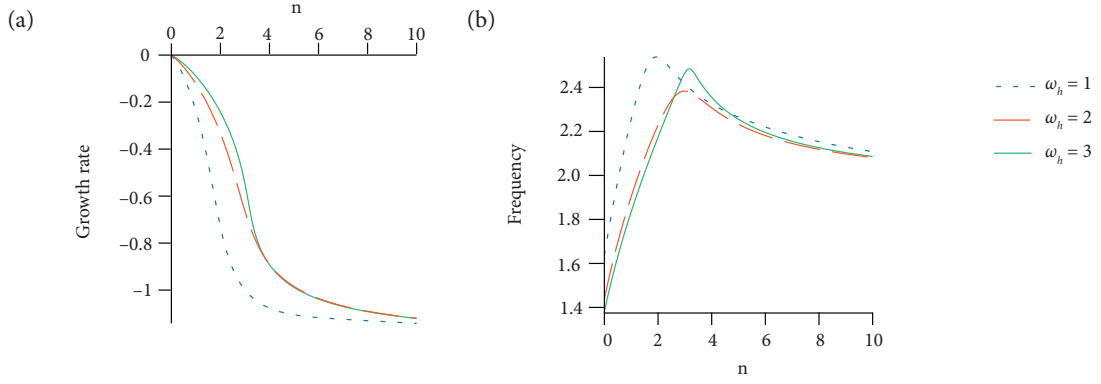

Figure 19. Thermoacoustic characteristics of a ducted resonator as resonator frequency varies (1L mode, $\tau = 0.6$, $x_f = 0.10$, $x_h = 0.5$, $V = 0.2$) showing (a) growth rate and (b) frequency.

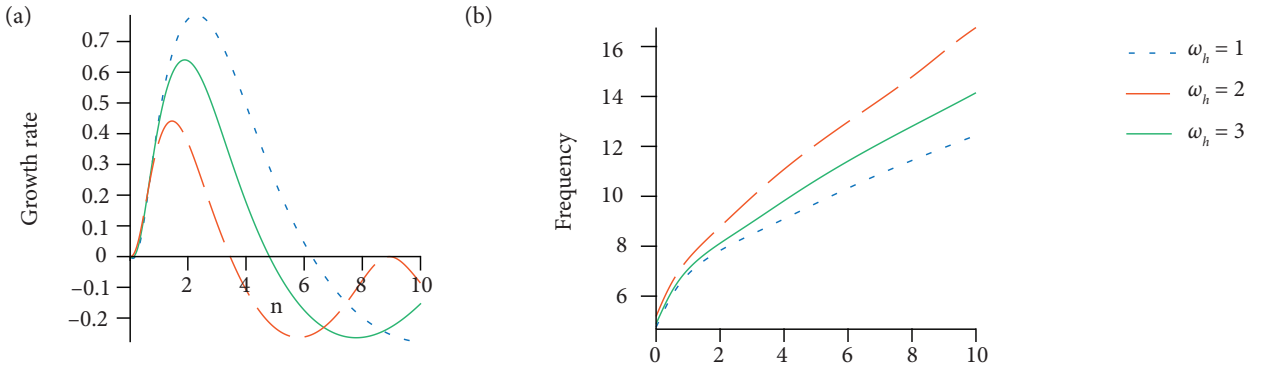

Figure 20. Thermoacoustic characteristics of a ducted resonator as resonator frequency varies (3L mode, $\tau = 0.6$, $x_f = 0.10$, $x_h = 0.5$, $V = 0.2$) showing (a) growth rate and (b) frequency.

notable changes due to variation in resonator frequency. The frequency diagrams for the 3L mode show that the rate of increase of frequency varies for different resonator frequencies and the highest rate of growth occurs at the highest resonator frequency. This indicates that improved coupling between the resonator and duct leads to faster modal transitions in the case of 3L modes.

SUMMARY AND CONCLUSIONS

The thermoacoustic characteristics viz. growth rate and frequency of 1L and 3L modes were plotted against combustion gain for different combustion delay and geometric parameters using a mode tracking algorithm. Nominal parameters were fixed for relevance to liquid propulsion and to bring out the effect of resonator geometry and position. Effect of variation of parameters was investigated one at a time.

The 1L and 3L modes were seen to have behavior in the nominal condition, which was of opposite nature at low combustion gain, i.e. low mixture ratio. The 1L mode was stable in the nominal condition whereas the 3L mode had a significant unstable segment. At higher mixture ratios (below stoichiometric) the 3L mode also stabilized. Hence the analysis predicts thermoacoustic instability for lean mixtures, which is also seen in practical combustors.

The frequency mode diagram typically shows transitions to higher frequencies than the original mode. These transitions are seen to be correlated to the changes in the trends of the growth rate mode diagrams.

In both duct and ducted resonator, there exists an optimum combustion delay for maximum stability in the case of 1L mode and for maximum instability in the case of 3L mode at lower mixture ratios.

Introduction of a resonator completely stabilizes the 1L mode when the standoff distance of the flame from the injector head is larger. Such a complete stabilization is not observed in the 3L mode.

Effect of increasing the volume of resonator is destabilizing for the 1L mode and stabilizing for the 3L mode up to a combustion gain of about 7. Thereafter, increasing the volume ratio is destabilizing for both.

Position of resonator for maximum stabilization of the 3L mode has an optimum, which is near the antinode of the corresponding standing wave pattern, in the duct as would be expected. For the 1L mode, the resonator should be close to the exit of the duct for maximum stabilization. Again, this corresponds to the antinode of the standing wave pattern.

When the characteristic frequency of the resonator and the mode frequency are close to each other, maximum stabilization occurs both for 1L and 3L modes, which agrees with experimental observation.

The results of the analysis show that volume variable resonators can be used to control thermoacoustic instability in open loop for selected modes. Multiple resonators with different geometric parameters would be required for simultaneous control of more than one mode.

AUTHOR'S CONTRIBUTION

Conceptualisation, Thannickal VM; Methodology, Thannickal VM and Tharakan TJ; Investigation, Thannickal VM; Writing – Original draft, Thannickal VM; Writing – Review and Editing, Tharakan TJ, and Chakravarthy SR; Resources, Thannickal VM; Supervision, Chakravarthy SR.

REFERENCES

Annaswamy AM, Ghoniem AF (2002) Active control of combustion instability: theory and practice. IEEE Control Syst 22(6):37-54. https://doi.org/10.1109/MCS.2002.1077784

Bedout JM, Franchek MA, Bernhard RJ, Mongeau L (1997) Adaptive-passive noise control with self-tuning Helmholtz resonators. J Sound Vib 202(1):109-123. https://doi.org/10.1006/jsvi.1996.0796

Chen LS, Bomberg S, Polifke W (2016) Propagation and generation of acoustic and entropy waves across a moving flame front. Combust Flame 166:170-180. https://doi.org/10.1016/j.combustflame.2016.01.015

Corá R, Martins CA, Lacava PT (2014) Acoustic instabilities control using Helmholtz resonators. Appl Acoust 77:1-10. https://doi.org/10.1016/j.apacoust.2013.09.013

Crocco L (1965) Theoretical studies on liquid-propellant rocket instability. Symposium (International) on Combustion 10(1):1101-1128. https://doi.org/10.1016/S0082-0784(65)80249-1

Dowling AP, Morgans AS (2005) Feedback control of combustion oscillations. Annu Rev Fluid Mech 37:151-182. https://doi.org/10.1146/annurev.fluid.36.050802.122038

Estève SJ, Johnson ME (2005) Adaptive Helmholtz resonators and passive vibration absorbers for cylinder interior noise control. J Sound Vib 288(1-4):1105-1130. https://doi.org/10.1016/j.jsv.2005.01.017

Harrje D, Reardon F, editors (1972) Liquid propellant rocket combustion instability. (NASA-SP-194). NASA Technical Report.

Jacobsen F (2000) Propagation of sound waves in ducts. Ørsted: Technical University of Denmark.

Li J, Morgans AS (2015) Time domain simulations of nonlinear thermoacoustic behaviour in a simple combustor using a wave-based approach. J Sound Vib 346:345-360. https://doi.org/10.1016/j.jsv.2015.01.032

Lieuwen TC, Yang V, editors (2005) Combustion instabilities in gas turbine engines (operational experience, fundamental mechanisms and modeling). Reston: AIAA.

McManus KR, Poinsot T, Candel SM. A review of active control of combustion instabilities. Prog Energy Combust Sci 19(1):1-29. https://doi.org/10.1016/0360-1285(93)90020-F

McManus KR, Vandsburger U, Bowman CT (1990) Combustor performance enhancement through direct shear layer excitation. Combust Flame 82(1):75-92. https://doi.org/10.1016/0010-2180(90)90079-7

Oefelein JC, Yang V (1993) Comprehensive review of liquid-propellant combustion instabilities in F-1 engines. J Propuls Power 9(5):657-677. https://doi.org/10.2514/3.23674

Olgac N, Zalluhoglu U, Kammer AS (2014) Predicting thermoacoustic instability: a novel analytical approach and its experimental validation. J Propuls Power 30(4):1005-1015. https://doi.org/10.2514/1.B35162

Richards GA, Straub DL, Robey EH (2003) Passive control of combustion dynamics in stationary gas turbines. J Propuls Power 19(5):795-810. https://doi.org/10.2514/2.6195

Sattinger SS, Neumeier Y, Nabi A, Zinn BT, Amos DJ, Darling DD (2000) Sub-scale demonstration of the active feedback control of gas-turbine combustion instabilities. J Eng Gas Turbines Power 122(2):262-268. https://doi.org/10.1115/1.483204

Sewell JB, Sobieski PA (2005) Monitoring of combustion instabilities: Calpine's experience. In: Lieuwen TC, Yang V, editors. Combustion instabilities in gas turbine engines (operational experience, fundamental mechanisms and modeling). Reston: AIAA. p. 147-162.

Surendran A, Hosseini N, Teerling OJ, Heckl MA (2016) Use of heat exchanger for passive control of combustion instabilities. Presented at: 23rd International Congress on Sound and Vibration; Athens, Greece. https://doi.org/10.13140/RG.2.2.10298.18881

Williams JEF (1984) Review lecture: anti-sound. Proc R Sound Lond A 395:63-88. https://doi.org/10.1098/rspa.1984.0090

Yang D, Morgans AS (2016) A semi-analytical model for the acoustic impedance of finite length circular holes with mean flow. J Sound Vib 384: 294-311. https://doi.org/10.1016/j.jsv.2016.08.006

Yang V, Andersen WE, editors (2000) Liquid rocket engine combustion instability. Reston: AIAA.

Yu K, Trouve A, Candel S (1991) Combustion enhancement of a premixed flame by acoustic forcing with emphasis on role of large-scale vortical structures. Presented at: 29th Aerospace Sciences Meeting; Reno, USA.

Zalluhoglu U, Olgac N (2016) Placement of Helmholtz resonators in series for passive control of thermoacoustic instabilities from a time-delay perspective. Presented at: 2016 American Control Conference (ACC); Boston, USA. https://doi.org/10.1109/ACC.2016.7525187

Zhang Z, Zhao D, Han N, Wang S, Li J (2015) Control of combustion instability with a tunable Helmholtz resonator. Aerosp Sci Technol 41:55-62. https://doi.org/10.1016/j.ast.2014.12.011

Zhao D, Morgans AS (2009) Tuned passive control of combustion instabilities using multiple Helmholtz resonators. J Sound Vib 320(4-5):744-757. https://doi.org/10.1016/j.jsv.2008.09.006